Short Circuit Signatures from Different Wind Turbine Generator Types

Jorge Martínez, Philip C. Kjær, Pedro Rodriguez, Member, IEEE, Remus Teodorescu, Senior Member, IEEE.

***Abstract*— Modern wind power plants are required and designed to ride through faults in the network, subjected to the fault clearance and following grid code demands. Beside voltage support during faults, the wind turbine fault current contribution is important to establish the correct settings for the relay of the protections.**

The following wind turbine generator during faults have been studied: (i) induction generator, (ii) induction generator with variable rotor resistance (iii) converter-fed rotor (often referred to as DFIG) and (iv) full scale converter.

To make a clear comparison and performance analysis during faults, and the consequent effects on substation protections, the aforementioned configurations have been simulated using PSCAD/EMTDC, with the same power plant configuration, electrical grid and generator data.

Additionally, a comparison of these wind turbine technologies with a conventional power plant, with a synchronous generator, has been simulated.

This paper addresses the difficulties that distance or overcurrent relays can experience when they are used in wind power plants. Whereas the short circuit contribution from power plants with synchronous generators can be calculated on the basis of the machine parameters alone, for wound rotor asynchronous and full scale generators power plants, the converters or rotor circuitry representation have to be taken into account for short circuit current studies and relay settings.

***Index Terms*—Wind turbine generator, power system, faults, doubly fed generator, full scale converter, short circuit currents, distance relays.**

I. Nomenclature

C	Capacitor
CB	Circuit Breaker
CT	Current Transformer
DC,AC	Direct Current, Alternate Current
DFIG	Doubly Fed Induction Generator
FSC	Full Scale Converter
G	Generator
IG	Induction Generator
IGR	Induction Generator with Rotor resistances
LV	Low Voltage
P, Q	Active, Reactive power
PCC	Point of Common Coupling
PI	Proportional and Integer
S	Apparent power
SG	Synchronous Generator
SCR	Short Circuit Ratio
SET, SCL	Substation, Short Circuit Level
V, I	Voltage, Current
OVL	Overhead Line
WPP, WTG	Wind Power Plant, Wind Turbine Generator
WPPT	Wind Power Plant Transformer
WTGT	Wind Turbine Generator Transformer
ω	Angular frequency
X, R	Inductance, Resistor
Z	Impedance

Subscripts

a, b, c	Three phase quantities
d, q	Direct and quadrature axes
ref	Reference
m	Measured

Manuscript September 10, 2010.

J. Martínez and P. C. Kjaer are with VESTAS Wind System.
R. Teodorescu and P. Rodriguez are with Aalborg University.

978-1-61284-788-7/11/$26.00 ©2011 IEEE

II. Introduction

With increasing penetration of wind power generation, the requirements for the connection of wind power plants (WPPs) to the electrical grid are defined by the new and emerging grid connection codes. The grid connection requirements vary in different parts of the world, but they have some common aims, like permitting the development, maintenance and operation of a coordinated, reliable and economical transmission or distribution system. The new requirements generally demand that WPPs provide ancillary services to support the network in which they are connected [1]-[2]. Wind turbine technology is evolving from the direct connected induction generator (IG) or doubly fed induction generator (DFIG) to the full scale converter (FSC) with either IG or SG, where better controllability of the current output can be achieved.

These different technologies used in WPPs provide very different short circuit current signatures, which should influence the protection settings of the WPP. Whereas the fault current in the case of a SG can be calculated based on the generator and the fault impedances, this can not be done with some of the WTGs, i.e., the DFIG and IGR technologies as a consequence of the dissipated energy in the rotor excitation during faults, and in the FSC technology since the stator is connected to the grid via AC/DC DC/AC converters. These WTGs are controlled during faults in a manner that leads to a behavior quite different from the SGs.

III. Wind turbine generator types

Most of the used wind turbines employ one of the electric-mechanical energy conversion schemes depicted in Fig. 1, 2, 3 and 4. In the following, a brief explanation about these technologies can be found.

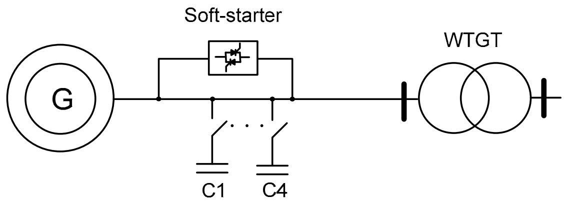

Fig. 1. IG; fixed speed cage induction generator.

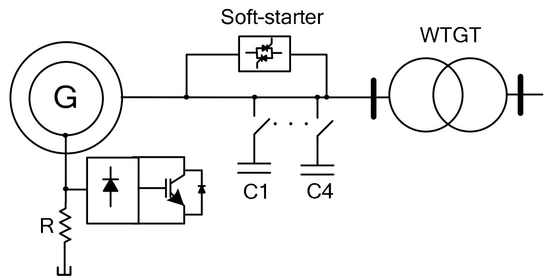

Fig. 2. IGR; variable speed wound rotor asynchronous generator with variable rotor resistance.

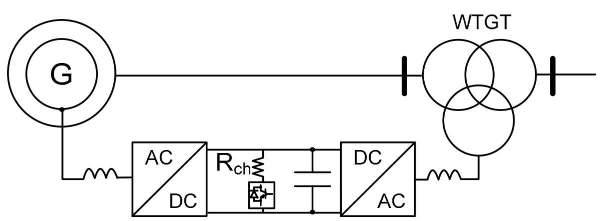

Fig. 3. DFIG; variable speed doubly fed generator.

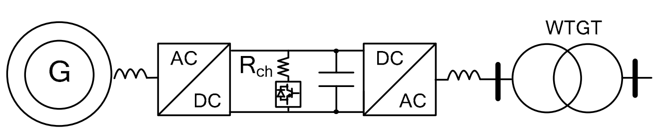

Fig. 4. FSC; variable speed full scale conversion.

A. IG

The fixed-speed squirrel-cage induction generator, Fig. 1, requires a soft starter for being connected to grid, and employs capacitor banks (in this case 4 steps are represented) for power factor correction, i.e., to compensate the generator reactive power consumption. The generator electrical torque is not directly controlled.

B. IGR

The variable rotor resistance wound rotor asynchronous generator is a variable speed generator, Fig. 2, and allows adaptation of the generator torque-slip curve to wind conditions, in order to maximize the energy extraction. The effective rotor resistance (R) is controlled by a power electronic circuit involving a chopper switch. By adjusting the duty cycle of the switch, the effective resistance applied to the rotor circuit can be dynamically controlled. Therefore, the torque can be controlled to achieve the desirable performance [3].

Soft starter and power factor correction circuitry are still needed, as for the case of the IG.

A simple diagram of the controller is shown in Fig. 5, where it can be seen how the duty cycle of the switch is calculated based on two cascade PI controllers. A look-up table, with the generator speed as an input, is used to generate the active power reference (P_{ref}).

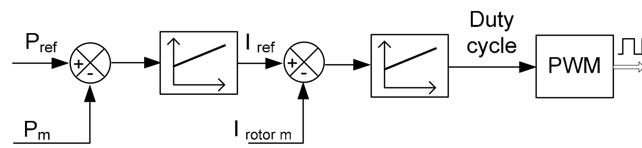

Fig. 5. IGR simplified diagram controller.

C. DFIG

The variable speed doubly-fed generator, Fig. 3, allows full control of generator active and reactive power using the rotor-connected frequency converter. Its rating is in the order of 0.3 pu. Operating both with sub- and super-synchronous speed the power can be fed both in and out of the rotor circuit. The rotor connected converter can employ various power dissipation solutions (sometimes referred to as active crowbar located in the rotor terminals or chopper located in the DC link bus bar: (R_{ch}). The simplified control of the rotor converter is depicted in Fig. 6, where the active and reactive power are controlled using the d and q axes respectively.

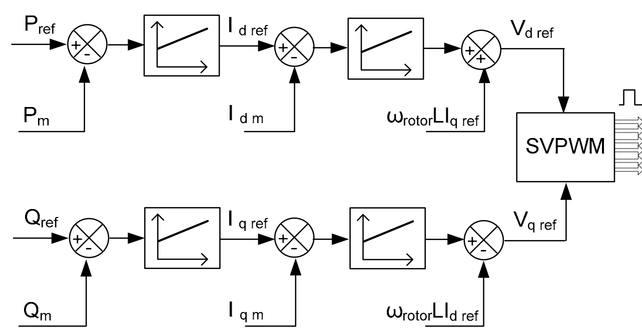

Fig. 6. DFIG simplified diagram controller

D. FSC

With the full scale converter WTG, all the power goes through the back to back power converter, the generator (this could be IG or SG) is effectively decoupled from the grid. The generator power can be dissipated in the converter DC link by means of a brake resistor (R_{ch}), see Fig. 4. Reaction to the grid faults will be dependant on the grid converter rating and its control. In Fig 7 it can be seen a simplified diagram of the control of the converter connected to the grid-side, which is the one of interest.

The d axis loop controls the DC-link voltage level, and the q axis loop controls the reactive power supplied to the grid.

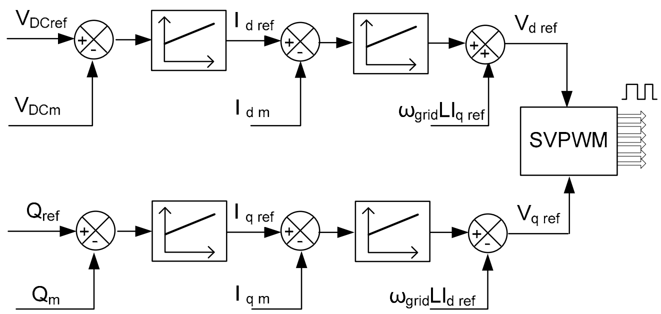

Fig. 7. FSC simplified diagram controller

IV. Case Setup

The following cases have been simulated in PSCAD with a simulation time step of 50 μs. The same base set-up case has been used with the four different WTG models mentioned in section III. See Fig. 8 for the set-up of the base case.

In every case, the WTGs composing the WPP are represented as an aggregated one. This aggregated WTG is connected through its set-up transformer to the collector bus by means of a subterranean cable. This collector bus is step-up to the high voltage level, by means of the substation transformer, WPPT in Fig. 8. The high voltage terminal of this transformer is connected to the next substation through an overhead line. Upstream of this point the whole electrical system is reduced to an equivalent, defined by its SCR and angle.

The subterranean feeder cables are modeled as a PI equivalent, with an X/R ratio of a 240 mm^2 section cable and a total impedance of 1 % (Z_{cable}). The OVL is modeled as a PI equivalent, with the X/R ratio of a 150 mm^2 section OVL, and with a total impedance of 2 % (Z_{OVL}). The substation and WTG transformers are modeled with 12 % and 8 % impedance, and an X/R ratio of 24 and 10 respectively. See more data simulation details in the appendix tables.

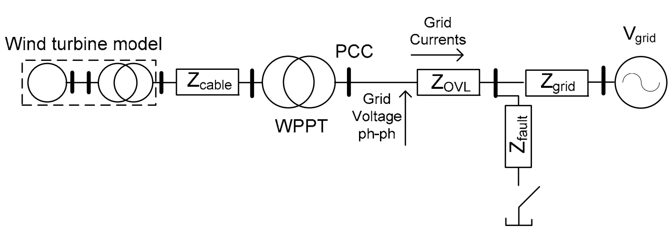

Fig. 8. Simulated base-case system diagram.

The grid is represented by an equivalent Thevenin circuit with a SCR of 10 and an angle of 75 degrees (Z_{grid}). The impedance to the fault (Z_{fault}) is calculated accordingly to make a voltage divider with the desired ratio. The fault is applied after the OVL, following the scheme depicted in Fig. 8.

V. Protection Short Circuit Current Coordination

Modern WPPs are required and designed to ride through faults in the transmission and distribution networks, subjected to fault clearing.

Fig. 9 represents a typical OVL protection system for a WPP with a radial connection, where a distance relay (21), which basically would trip for faults up to a certain distance away from a substation but not beyond that point, and an earth directional overcurrent (67N) protection relay are used. ANSI device numbers are used for the representation of the relays [4].

In Fig. 9 only the relay functions at PCC related to OVL protection have been plotted.

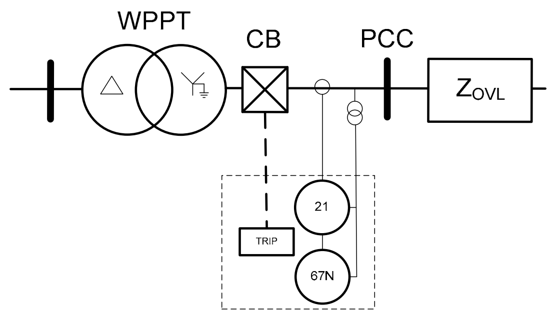

Fig. 9. OVL current protection diagram.

VI. Simulation Results

In the following, each of the generator types, shown in section III, has been subjected to a simulated 3-phase bolted short circuit. The test circuit used in the simulations is shown in Fig. 8. In all of the following simulations the residual voltage at PCC is 0.1 pu, the pre-fault active power is 1 pu, and the power factor is 1 at WTG terminals. The fault is cleared after 500 ms.

In the following simulations, 3-phase short circuits are applied at time 0 seconds. The voltages and currents seen at PCC during the simulations are shown.

In all the simulated cases, the current and voltage waveforms have been processed using a sixteen samples cycle, full cosine cycle filter algorithm, as it is particularly suited for protective digital relaying, while extracting the fundamental, the filter rejects all harmonics including the decaying exponential [5].

The following figures show the instantaneous 3-phase values of the real (blue color line) and processed data (red color line), as well as the envelope of the instantaneous 3-phase values of the real (solid blue line) and processed data (dashed red line) of the voltages and currents at PCC. The used indexes in the figures, for the instantaneous and the envelope of the instantaneous data, are: $_{abc}$ and $_{envelope}$ respectively.

A. IG

As the squirrel-cage induction generator is uncontrolled, it sources a large reactive current and demagnetizes based on generator and grid impedances. Upon the recovery of the line voltage, the re-magnetization of the generator will sink a large reactive current. See Fig. 10.

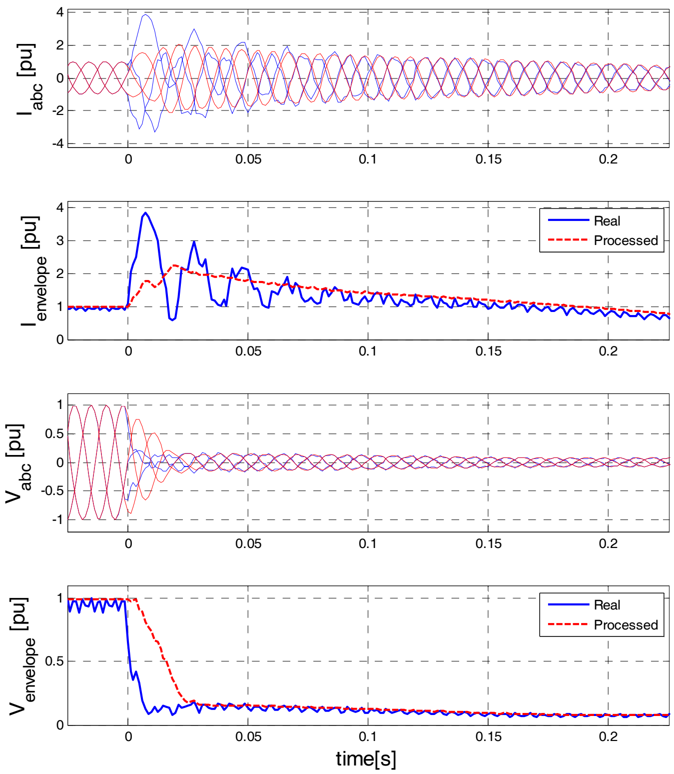

Fig. 10. 3-phase fault, IG case.

B. IGR

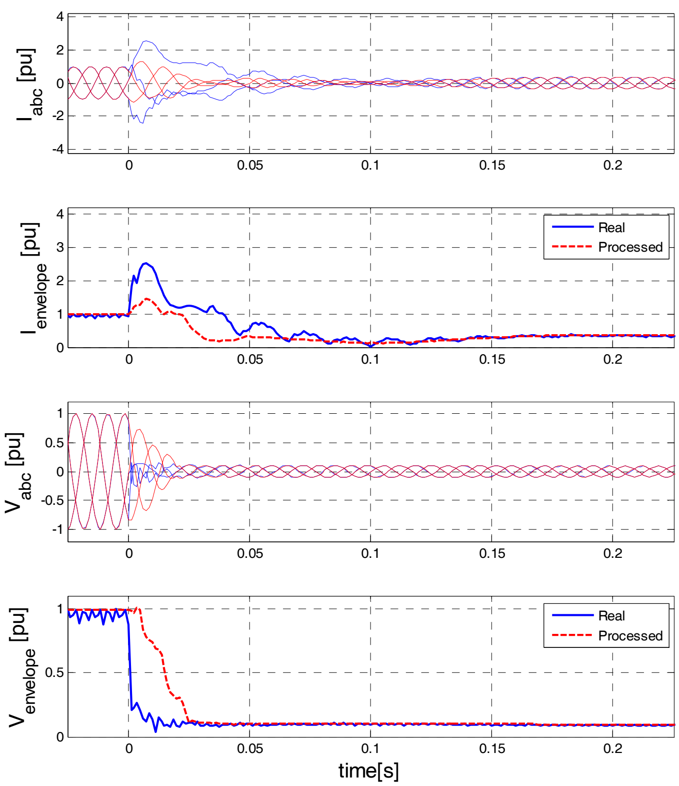

Fig. 11. 3-phase fault, IGR case.

Upon the rise of the stator current, the rotor current will exceed its reference value, I_{ref} in Fig. 5, and the power electronic switch is continuously off, leading to the maximum rotor resistance value, necessary for limiting the rotor current. This causes a rapid dissipation of energy as the generator demagnetizes.

The resulting stator currents exhibit a much lower AC component than in the case of the squirrel cage induction generator.

Once the rotor current falls below its reference value from pre-fault operation, the power electronic switch can actively modulate the effective rotor resistance again, and can bring the current back to its reference value (subject to limitations by stator voltage range restrictions). See Fig. 11.

C. DFIG

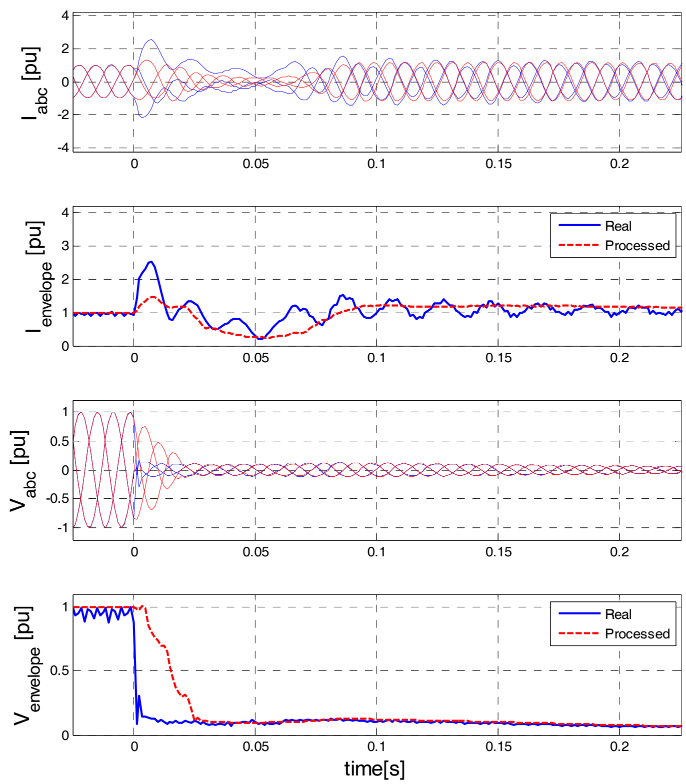

Fig. 12. 3-phase fault, DFIG case.

DFIG technology can present different short circuit current response depending on the fault severity. Usually, for severe faults the rotor converter is blocked during certain time to protect itself against high currents. Upon the rise of the stator current, the rotor current forces the rotor connected converter to block and its diodes to freewheel, which charges the DC link rapidly.

The brake chopper maintains the DC voltage level by turning on the DC link chopper in full conduction mode (no chopping). Once the rotor currents fall below their protection levels, the rotor-connected converter resumes switching and the rotor windings are subjected to a controlled voltage, which will cause the injection of reactive current according to the stator voltage level.

The I_q reference is calculated according to the stator voltage (V_{LV}) and usually it is defined by the grid codes, see Fig. 13. Thus, the WTG supports the grid voltage recovering process [6-8]. The I_q current compoenet during the fault can be seen in Fig. 18.

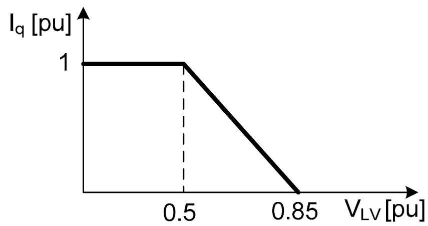

Fig. 13. I_q reference according to the stator voltage.

D. FSC

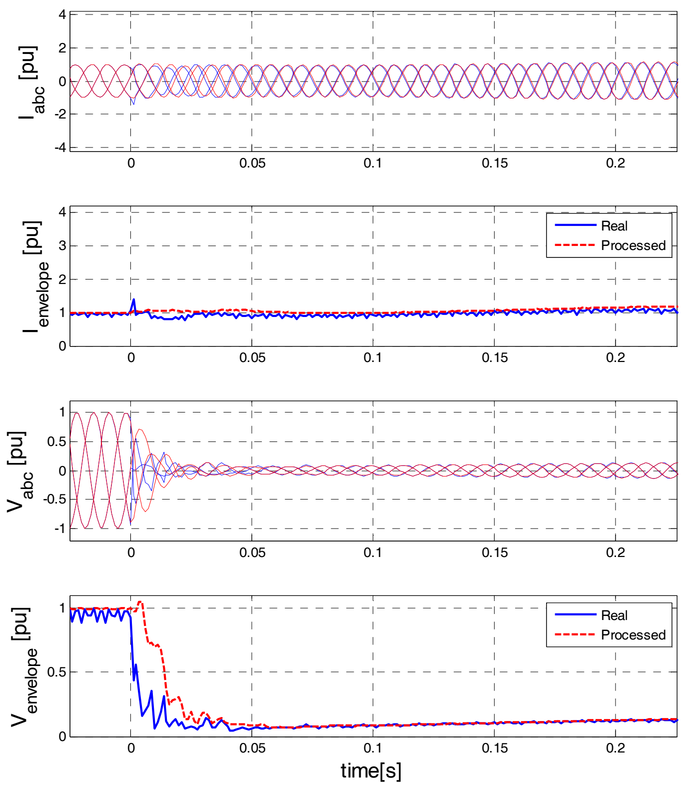

Fig. 14. 3-phase fault case FSC.

The grid connected converter could have several behaviors depending on the sizing of the electronics, control capabilities and fault severity, i.e. the following two cases are presented: (i) the grid converter blocks its switching upon over-current limit, and then resumes switching action to produce 1 pu or other reactive current level, (ii) the grid converter blocks switching during the entire fault period [9].

Only the case (i) is shown in Fig. 14, due to the fact that the fault simulated is located at PCC, far away from converter terminals, having in between the converter terminals and fault location: the subterranean cable, the OVL, the WTG and the WPP transformers impedances, therefore, reducing the risk of reaching high peak current values.

As can be seen in Fig. 18 the FSC will inject 1 pu I_q, as fast as the control is ready (it can be said that the transient is a control transient and not an electromagnetic transient, lasting only several ms), according to the reference calculated upon the stator level (V_{LV}). See Fig. 12.

E. SG

In this case, a synchronous generator with round rotor and one damping circuit has been tuned to have similar response than the short circuited generator used in the other cases [10].

This has been done to compare the previous cases with a conventional power plant with a synchronous generator.

The SG shows during the fault, see Fig. 15, a fundamental frequency oscillatory component, due to interaction with the rotor field, and a unidirectional component caused by the fundamental frequency induced in the rotor. Generator and grid inductances will dictate the rotor and stator current decay times.

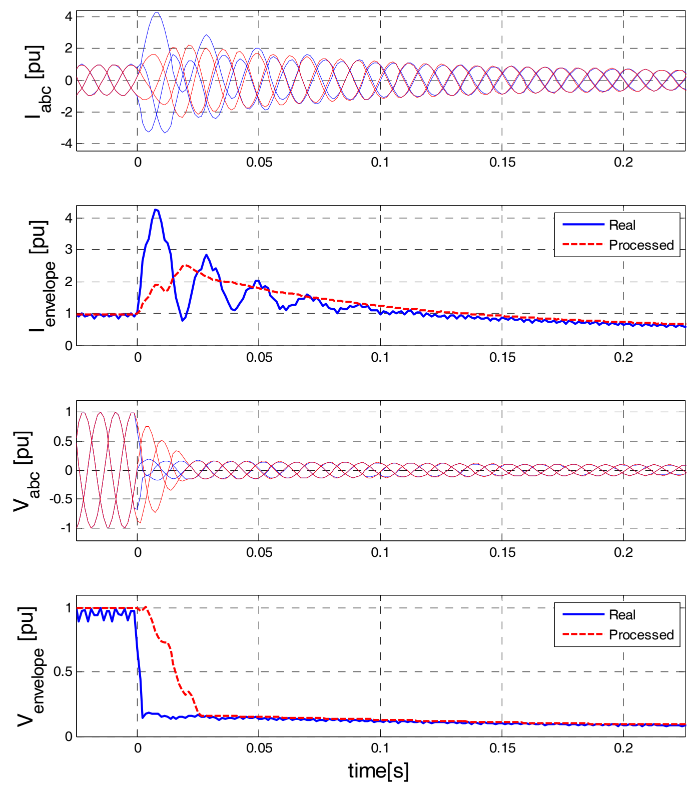

Fig. 15. 3-phase fault, SG case.

VII. Impedances to the Fault and Maximum Peak Current Values

A list of the different maximum peak values obtained in the simulated cases are depicted in table 1, as well as a comparison of these peak values with the one obtained for the SG.

TABLE I
MAXIMUM SHORT CIRCUIT PEAK CURRENTS

	IG	**DFIG**	**IGR**	**FSC**	**SG**
I_{peak} [pu]	*3.9*	*2.5*	*2.5*	*1.4*	*4.2*
I_{peak} relative to SG [pu]	*0.93*	*0.61*	*0.61*	*0.33*	*1.00*

Voltages and currents extracted from the previous cases have been processed using the sixteen samples cycle, full cosine cycle filter algorithm [11]. With these values, the different impedances to the fault ($Z_d = V/I$) are calculated and shown in Fig. 16.

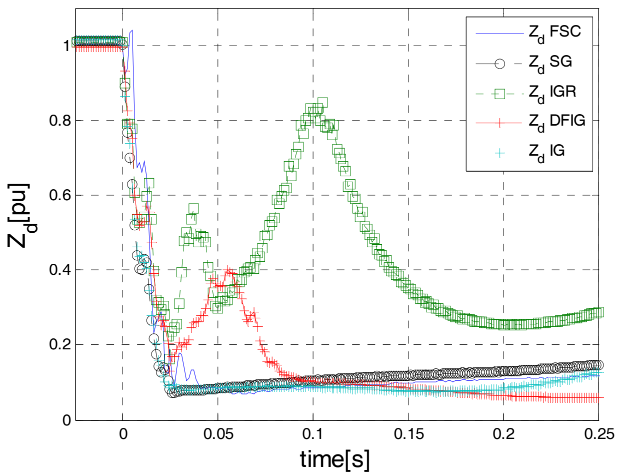

Fig. 16. Impedance to the fault for the different WTGs.

VIII. Analysis of the Results

As the waveforms in the previous graphs demonstrate, the short circuit contribution from different turbine technologies, using the same generator but different circuitry attached to the rotor or stator, vary widely.

Generally speaking;

a) The IG and the SG behave similarly, as they both preserve the rotor field well into the duration of the fault. Therefore, they exhibit very similar current to the fault, showing high peak currents and high AC current component.

b) The IGR and the DFIG both dissipate significant power on the rotor side during faults, and therefore shorten the rotor decay times, which implies the following: reduced peak currents, and lower AC current components. This low AC component could lead to a bad function of the distance relays when classifying the zone where fault is located (as it can be seen in Fig. 16). Using differential relays should be considered instead of distance relays. Moreover, this low AC component could be a problem for the breaker operation when trying opening currents at non zero crossing, saturation of the CTs, due to the current DC component, should be a concern as well.

c) The FSC separates itself by virtually no difference between nominal and short circuit current amplitude. Short circuit current will be dependant on control and converter sizing. This technology exhibit low and short duration peak current during faults. In any case, the use of overcurrent relays could be a concern if the grid connected converter is blocked and consequently there is no current injection to the fault, or if it is not blocked and injects currents close to the rated value without any transient.

IX. Conclusions

WPPs comprise very different technologies compared to the SG power plants. The four most common wind turbine technologies (all of them using the same main electrical components: generator and transformer) and a SG with the same equivalent generator impedances have been subjected to a 3-phase fault showing that they exhibit very different short circuit current signatures.

The consequences of having quite different short circuit behavior than the SGs are shown when using distance or overcurrent protection relays.

DFIG and IGR technologies could lead to a malfunction of distance relays when detecting the zone where the fault is located, due to the low AC component in the injected short circuit currents, see Fig. 16. FSC technology could lead to problems when adjusting the overcurrent relays due to low short circuit peak values, additionally a permanent blocking of the converter will affect the correct distance relay operation too. See Table I.

Therefore, when there are not enough available data of the WTG circuitry and controls to make a proper short circuit study, the following combinations should be treated very carefully: DFIG-distance protection, IGR-distance protection and FSC-overcurrent protection.

For the DFIG, IGR and FSC, the circuitry attached to the rotor or stator of the generator and its control are influencing heavily the behavior during faults. Different control for same topology (same circuitry) could lead to different short circuit behavior, having the consequence that different manufacturers offering same topology could present different short circuit response.

As a conclusion, the WTG circuitry and its control should be represented correctly when studying short circuit currents from wind power plants, even in the cases of the DFIG or IGR where the converters represent only a small fraction of the total power. This shows the need of a standardization process for the WTG representation during faults and the importance of collecting the right data for short circuit studies for all WTG technologies.

X. Appendix

TABLE II
Electrical Data of Wind Turbine

Parameter	Value	Unit
S_{base}	2100	[kVA]
V_{base}	0.69	[kV]
Electrical frequency	50	[Hz]
Stator Resistance	0.006	[pu]
Rotor Resistance	0.009	[pu]
Mutual Inductance	3.422	[pu]
Stator Inductance	0.072	[pu]
Rotor Inductance	0.101	[pu]
S step-up transformer 0.69:20kV	2100	[kVA]
Z step-up transformer	0.08	[pu]

TABLE III
Electrical Data of the System

Parameter	Value	Unit
X_{cable}	0.65	[%]
R_{cable}	0.83	[%]
C_{cable}	1.66	[%]
X_{OVL}	1.81	[%]
R_{OVL}	0.89	[%]
C_{OVL}	0.51	[%]
X_{WPPT}	11.91	[%]
R_{WPPT}	0.49	[%]
X_{GRID}	9.66	[%]
R_{GRID}	2.58	[%]
High voltage level	115	[kV]

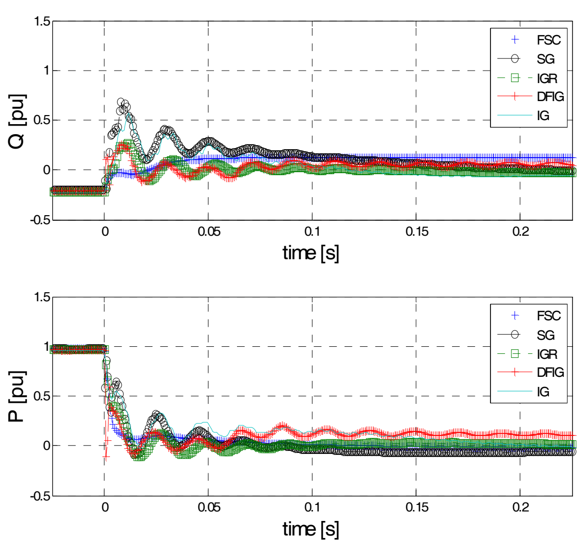

Fig. 17. P and Q at PCC for the different WTGs.

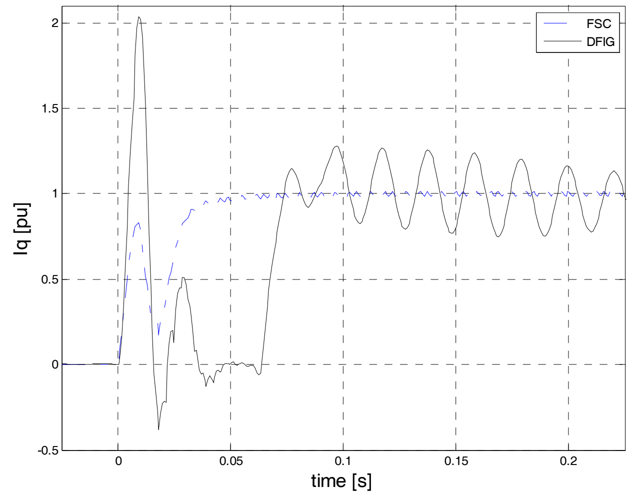

Fig. 18. Iq injected at LV for the FSC and DFIG.

XI. References

[1] P.O.12.3, "Requisitos de respuesta frenta a huecos de tension de las instalaciones de produccion de regimen especial", Royal Decree 436/2004, Red Electrica de Espana, July 2004, Grid Code Requirements for Voltage Dips in Spain.

[2] I. Erlich, U. Bachmann, "Grid Code requirements concerning Connection and Operation of Wind Turbines in Germany". IEEE Power Engineering Society General Meeting, 12-16 June 2005; 1253-1257 Vol.2.

[3] Liwei Wang, Sina Chiniforoosh, and Juri Jatskevich, "Simulation and Analysis of Starting Transients in Rotor-Chopper-Controlled Doubly-Fed Induction Motors" 2008 IEEE Electrical Power & Energy Conference.

[4] Applied Protective Relaying 1979 by Westinghouse Electric Corporation, 2nd Printing, "Appendix II, Electrical Power System Device Numbers and Functions" as adopted by IEEE standard and incorporated in American Standard C37.2-1970 and -2008.

[5] E.O Schweitzer III and Daqing hou, "Filtering for Protective Relay", 19th Annual Western Protective Relay Conference, Spokane, Washington, October 20-22, 1992.

[6] Johan Morren, Sjoerd W. H. de Hann, "Short-Circuit Current of Wind Turbines With Doubly Fed Induction Generator", IEEE Transactions on Energy conversion, Vol. 22, No. 1, March 2007.

[7] Morren J, de Haan SWH. "Ridethrough of Wind Turbines With Doubly-fed Induction Generator during a Voltage Dip". IEEE Transactions on Energy Conversion 2005; 20: 435–441.

[8] Ling Peng; Yongdong Li; Francois, B. "Dynamic behavior of doubly fed induction generator wind turbines under three-phase voltage dips". Power Electronics and Motion Control Conference, 2009. IPEMC '09. IEEE 6th International 17-20 May 2009 Page(s):620 - 626

[9] Conroy, J.F.; Watson, R. "Low-voltage ride-through of a full converter wind turbine with permanent magnet generator; Renewable Power Generation, IET Volume 1, Issue 3, September 2007 Page(s):182 - 189

[10] I.Boldea and S.A. Nasar: "Electric Machine Dynamics". Mac Millan Publishing Company. (July 1986), ISBN-10: 0029480302

[11] W.A. Elmore, C.A. Kramer, and S.e. Zocholl, "Effects of Waveform distorsion on Protective Relays". IEEE Transactions on Industrial Applications, Vol.29, No.2, March/April 1993, pp. 404-411.